

Lyudmila Nyrkova*, Anatolii Rybakov, Larysa Goncharenko,
Svetlana Osadchuk, Yulia Kharchenko

E.O Paton Electric Welding Institute of the National Academy
of Sciences of Ukraine, Kyiv, Ukraine

Scientific paper

ISSN 0351-9465, E-ISSN 2466-2585

<https://doi.org/10.5937/zasmat2302177N>



Zastita Materijala 64 (2)

177 - 189 (2023)

Analysis of the causes of fracture of the main gas pipeline

ABSTRACT

A complex of research has been conducted to establish the causes of the accident of the main gas pipeline made of 1420x15.7 mm X70 steel after 20 years of operation. It is found that pipe destruction was initiated by the longitudinal crack with a length of 470 mm and a maximum depth of 6.8 mm, oriented in the direction of the pipe and perpendicular to the outer surface of the pipe identified as stress-corrosion cracking. The crack initiation is due to the disboundment of the tape protection coating, the high corrosion activity of the soil, and the complex stress-strain state caused by deviations from the design objectives during construction. The chemical composition the base metal of all investigated pipes corresponds to the requirements of the technical conditions for steel pipes in category X70; pipes welding are performed with the typical materials used in pipe welding plants. Despite the differences, the structural and mechanical characteristics (yield strength, ultimate strength, and impact strength) of the steel and weld metal of the studied pipes are identical. The relative elongation (δ_5) of the operated pipes is below the normalized values, but, it is necessary to take into account the possibility of deviations in these characteristics of steel in the initial state. Significant reserves of toughness indirectly indicate low damage of metal and, accordingly, satisfactory resistance to destruction of the metal of the studied pipes.

Keywords: main pipeline, X70 steel, microstructure, mechanical properties, stress-corrosion cracking, cathodic protection

1. INTRODUCTION

The Ukraine's gas transport system (GTS) of includes a network of main gas pipelines and branch lines that create a single technological complex. Increasing the reliability of GTS operation is the most **critical** task in view of **extensive** lengths of gas pipelines, high gas pressure, long service life and natural and climatic conditions [1]. The main gas pipeline system significantly affects the environment's ecological state, which is especially manifested in accidents. The most dangerous phenomenon that is difficult to predict and prevent is stress corrosion cracking. The origination and propagation of this type of fracture reduce the stable operation of GTS.

The first stress-corrosion cracking (SCC) accompanied by an accident at main pipeline of 610 mm occurred 50 years ago in the United States of America [2].

Researchers around the world have described many similar fractures of main pipelines (Argentina, Australia, Canada, Iran, Iraq, Italy, the Netherlands, Pakistan, Saudi Arabia, Russia) [3-7]. The geography of spreading SCC at the beginning of the 1990s in the territory of the former USSR was limited to the northern regions. Later, failures caused by SCCs were registered in the sections of GTS in central regions, and in the early 2000s, cases of SCC were detected in its southern regions [2].

Today, it is known that stress corrosion defects originated and propagated on main gas pipelines, laid in the zone of spreading permafrost rocks. Previously, such a phenomenon was considered impossible. Damages to pipelines caused by stress-corrosion have expanded the boundaries not only in geographical but also in technological terms: stress-corrosion defects are revealed on connecting gas pipelines and main oil pipelines of a large diameter [8,9]. The experience of operating such structures shows that at the proper functioning of the cathode protection system, both on rectilinear as well as on spiral welded pipes with a film and rubber-bitumen insulation, in places of its

*Corresponding author: Lyudmila Nyrkova

E-mail: lnyrkova@gmail.com

Paper received: 01. 01. 2023.

Paper accepted: 31. 01. 2023.

Paper is available on the website: www.idk.org.rs/journal

defects and delaminations, propagation of SCC is possible [10]. In the problem zones of river floodplains and wetlands on those lines of main pipeline, where a large number of thin-walled double-welded pipes are laid, the activity of stress-corrosion process grows gradually.

In view of the abovementioned, the further work on the study of the mechanism of phenomena leading to the propagation of this type of fracture has an important scientific and practical role. The importance of a more detailed study of stress corrosion determines the relevance of conducting deep fundamental research and finding new approaches to determining the probability of its propagation.

2. EXPERIMENTAL

The chemical composition of the pipes was analyzed by the X-ray spectral method in the device "Spectrovak-1000" produced by the "Baird" company. The mechanical indices of the base metal and metal of welded joints were determined during the tension of the full-thickness specimens of the base metal and metal of welded joints at a rate of 6 mm/min in the ZDM machine. The impact energy was determined on the specimens of the base metal and metal of welded joints at temperatures of 20, 0, -20, -40, -60, and -100 °C in the KM 28 machine.

Metallographic sections were prepared according to the standard procedure. The structural characteristics of the base metal and metal of welded joints were estimated in the NEOPHOT 21 microscope at different magnifications on non-etched specimens and specimens after etching in a 4% nitric acid alcohol solution. The digital image was obtained using of the Sigeta UCMOS camera.

Slow strain rate tests were carried out on testing machine AIMA-5-1 at a rate of 10^{-6} s^{-1} . Plane specimens were subjected to tension in the air to the rupture in and in periodic wetting by solution. The test solution was NS4 solution of composition (g/l): 0.122 KCl + 0.483 NaHCO₃ + 0.137 CaCl₂ + 0.089 MgSO₄·7H₂O, pH 8.6. The periodicity of wetting the surface of specimens was established based on the analysis of the duration of maintenance of the raised level of ground waters in the territory of Ukraine in the spring-autumn period for 1 year. The periodicity of wetting was established as equal to 50 min in the solution and 10 min in the air. The cross-sectional area of the working part of specimens in the initial state was 30 mm². The tests were conducted at the potential of corrosion and the potentials of cathodic polarization of -0.75 V, -0.95 V, -1.05 V (relative to the chlorine-silver electrode of comparison).

Polarization curves were recorded in a potent dynamical mode according to a three-electrode scheme. In the tests the potentiostat PI-50-1.1, the programmer PR-8, and the recorder XY RECORDER A3 were applied. The scanning rate of the potential was 0.5 and 100 mV/s. As a working electrode, a specimen of a pipe steel served, as an auxiliary – platinum electrode, and as an electrode of comparison – saturated chlorine silver electrode (Ag/AgCl) was used.

3. RESULTS AND DISCUSSION

To find out the causes of the fracture of the main gas pipeline, a set of studies was conducted, which included:

- visual inspection of the fractured section and determination of the fracture site;
- determination of the chemical composition of the base metal, the metal of welded joints (factory longitudinal and circumferential site welds), and identification of grade of steel of the fractured pipes.
- determination of characteristics of strength, ductility, and impact toughness of the base metal of the pipes following the requirements of the specifications TS 14-3-995 [11] and BR 2.05.06 [12].
- determination of impact toughness and cold resistance (KCV) of the pipe metal near the fracture site and at some distance from it on Charpy specimens.
- determination of impact toughness (KCV) in the heat-affected zone of the longitudinal weld at different distances from the fusion line.
- metallographic examinations of structural features of the base metal, metal of the factory, and circumferential welded joints and metal near the fracture site;
- corrosion and mechanical studies of the base metal.

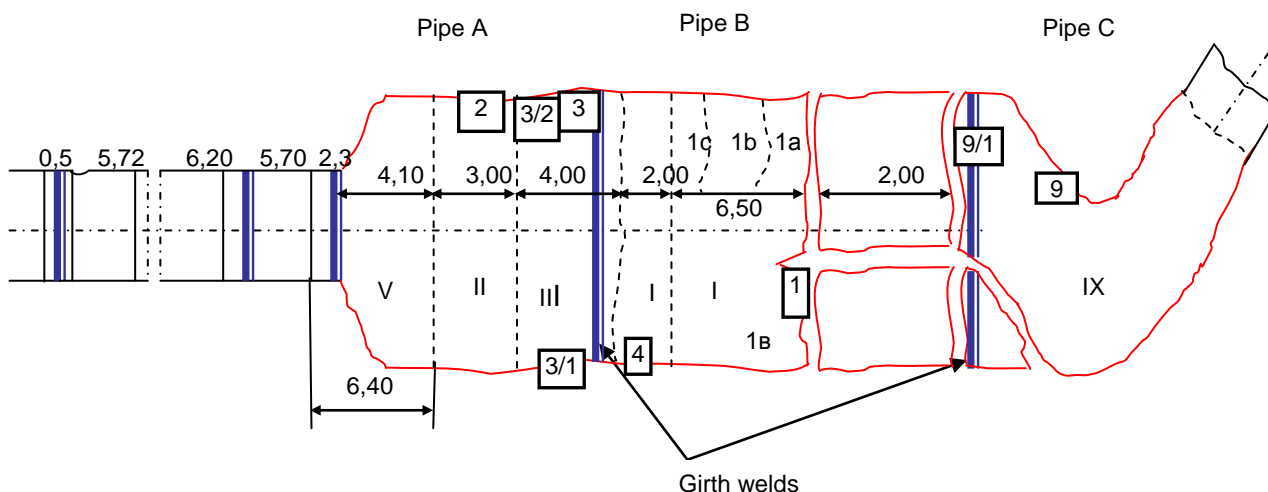
It should be noted that chemical composition and mechanical properties were determined for all the fractured pipes, but for a brief description in the article, the data for a pipe with a conditional marking A is given.

3.1. General information about the main gas pipeline

The main gas pipeline was commissioned in 1982. Analyzing the certificates for the pipes, it was found that the pipes were manufactured from the sheet steel of grade X70 of the controlled rolling of

the production of (Japan, France, Germany, and Austria) at the pipe plant of Ukraine following by TS 14-3-995 [11]. The pipes are double-welded and have a size of 1420x18.7 mm and 1420x15.7 mm. Gas pressure is 6 MPa. Within a radius of 1 km from the accident site, a highway and a power line with a voltage of over 30 kV are located. The

type of soil is loam and forest sandy loam, hard and semi-hard with a specific resistance (21-28) Ohm-m, pH 8.6. To protect against corrosion, the tape coating "Polyken 980-25" with a wrapping tape "Polyken 955-25" of (2+2) structure and electrochemical protection were used.



1, 2, 3, 3/1, 3/2, 4, 9, 9/1 – cites of selection the specimens for investigations
I, II, III, IV, V, IX – fragments of destroyed pipes for transportation; - breaking line

Figure 1. Scheme of the destroyed part of the main gas pipeline

Slika 1. Šema porušenog dela magistralnog gasovoda

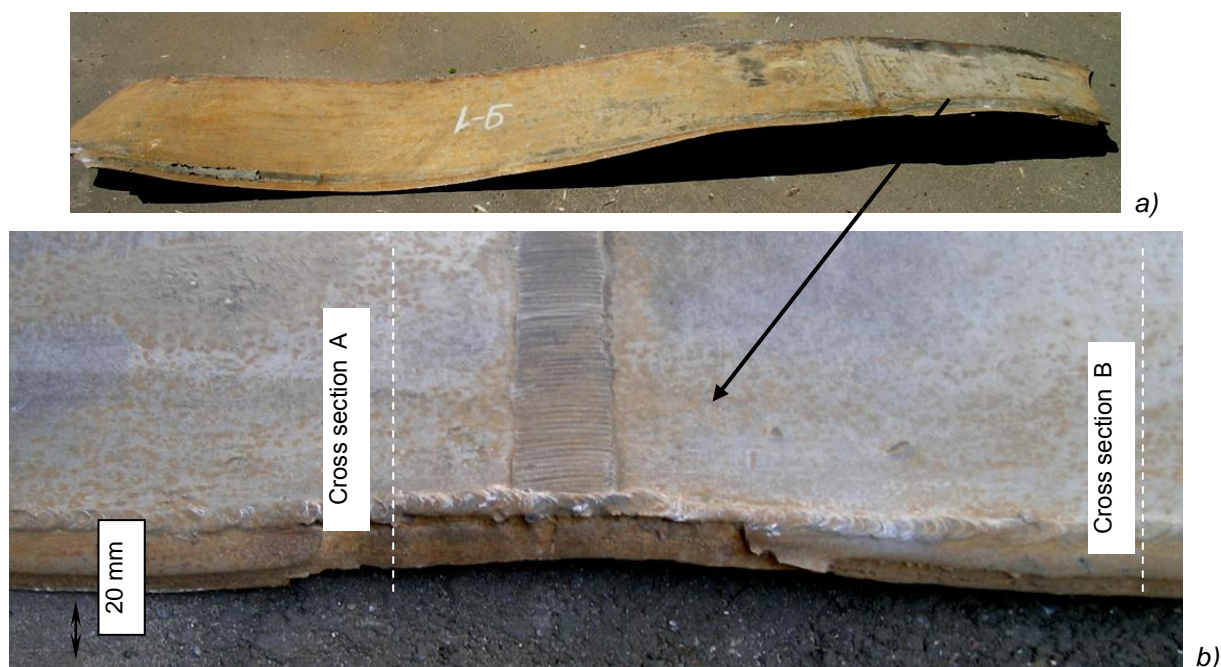


Figure 2. The fragment of the broken pipe C with girth weld joint (templet 9/1): a – appearance; b – region near the fracture edge along the fusion line of girth weld

Slika 2. Fragment prelomljene cevi C sa prstenastim zavarenim spojem (templet 9/1): a – izgled; b – oblast u blizini ivice loma duž linije spajanja prstenastog zavara

3.2. Results of visual inspection of the fracture site

As a result of the inspection of the accident site, it was found that 3 pipes conditional markings A, B, and C were fractured (Fig. 1). The crack propagated along pipe A and the section of pipe C to about 8.5 m length and changed its direction to the circumferential. Further, pipe B in the section of about 2 m in length was ruptured into two semi-cylinders as a result of the formation of two cracks, and after crossing the circumferential weld between pipes B and C, two cracks passed on a spiral line. Pipes A and B were for some time in the area of gas burning.

The fracture of the pipes occurred in the direction of the generatrix of the gas pipeline at a distance of 0-20 mm (fragments 2, 3, 3/1, 3/2), and at a distance of 30-60 mm from the fusion line of the longitudinal weld (templet 4). On one of the pipes (templet 9/1), the rupture line passed at a distance of ~25 mm from the circumferential weld, and on the section of ~130 mm length, it passed at a distance of 2 mm from the fusion line of the circumferential weld (Fig. 2), intersected the root layer of the circumferential weld and extended over the heat-affected zone of the backup layer (Fig. 3).

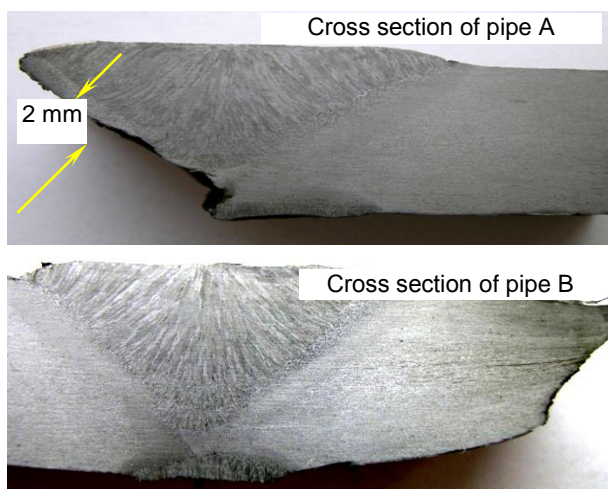


Figure 3. Macrosection of girth weld joint (specimen 9/1)

Slika 3. Makrorez prstenastog zavarenog spoja (uzorak 9/1)

For investigations, the specimens were selected in the sections where based on the results of the preliminary inspection, cracking of the gas pipeline could be initiated Fig.2 (specimens 2, 3, 3/1, 9/1). Also, the specimens for determination of mechanical properties and structural features of the metal (specimens 3/2, 4, 9) were selected.

The circumferential weld was produced by manual arc welding applying the technology used

at the time. Defects of welding origin in the facing layer were not detected. There were separate minor defects in the root layer: slag inclusions (up to 0.5 mm in size) and lack of fusion (from 1 to 2 mm depth, exceeding the permissible value (1 mm according to HS&R III-42)). The nature of the fracture, location of the section, and number and size of detected defects do not allow for considering this section as a probable fracture site.

On the surface of templat 2 and 3 of pipe A, at a distance of ~45 mm from the edge of the fracture, numerous crack defects of up to ~30 mm were found, which were oriented in parallel to the edge of the fracture (Fig. 4). The cracks are located outside the heat-affected zone. On specimens 4, 9, and 9/1 of pipes B and C, cracks on the outer surface are absent.

In specimen 3, a long crack (Fig. 5) with a length of ~470 mm and a maximum depth of ~6.8 mm is present, which was formed as a result of the coalescence of small cracks ~(12-30) mm long. A thinning of the pipe wall was detected, the maximum residual thickness of which was ~11.5 mm. The mentioned factors indicate an increased plastic deformation near the crack's edge, which may indicate the beginning of fracture.

A similar crack of ~130 mm in length and ~2 mm depth was revealed in templet 3 at a distance of ~400 mm from the first crack. On templet 2 of pipe A, cracks of the same character of ~ (80-90) mm length and from 2 to 5 mm depth were recorded (Fig. 5). In the fracture of other specimens (pipes B and C), cracks were not detected.

The fractured specimens 3, 3/1, 2, and 3/2 outside the cracking zone, including in a part of their final fracture, have predominantly a ductile layered nature, which alternates with a flexible type. Fracture in specimens 4, 9/1, and 9 has a flexible nature.

In the area of cracks and the other regions of fracture, the residual thickness of the pipe wall near the rupture line is ~(13-14.5) mm. In the area of fracture of the circumferential weld, the thickness of the pipe wall decreases to ~(11.2-12.5) mm. The thickness of the walls of pipes A, B, and C in the sections distant from the edge of the fracture is (15.4-15.5) mm, which corresponds to the rated thickness of the wall of the fractured pipes – 15.7 mm.

During the exterior inspection of the surface of longitudinal welded joints, defects of welding origin in the welds of the pipes were not detected.



Figure 4. The fragment of broken pipe A (templet 2): a – appearance; b – cracks near the broken edge; c, d – stratification in the rupture

Slika 4. Fragment slomljene cevi A (templet 2): a – izgled; b – pukotine u blizini slomljene ivice; c, d – raslojavanje u rupturu

The formation of both longitudinal and circumferential welds is satisfactory with a smooth transition to the base metal. The height of the reinforcement of the outer welds in the factory and circumferential welded joints is within $\sim(2.5-2.8)$ mm and $\sim(2.0-2.5)$ mm, which meets the requirements of BR 2.05.06 and BR III-42.

Thus, it can be assumed that the fracture of the pipes on the section of the gas pipeline was initiated by a crack defect of ~ 470 mm in length with a maximum depth of ~ 6.8 mm, detected in the fracture in the direction of the generatrix of the pipe A at a distance of ~ 20 mm from the fusion line of the longitudinal weld of the pipe.

3.3. Identification of the chemical composition

Chemical composition. As to the chemical composition (Table 1), the pipe metal belongs to the low carbon steel microalloyed by vanadium and niobium and corresponds to the standard documents to the steel of category X70.

The mass fraction of elements in the metal of inner and outer welds is typical for welds produced with the use of welding wires

Sv-08GNM and Sv-08GM and a high-silicon flux of AN-60 type, which is usually used at the factory during the manufacture of pipes.

3.4. Mechanical properties of base metal, longitudinal and circumferential welded joints

According to the results of determining the mechanical properties, as to the standard indices (σ_y , σ_t , σ_y/σ_t , δ_5 , KCV^{15}), the base metal of the fractured semi-cylinder of pipe A (Table 2) meets the requirements of TS 14-3-995 [11] and BR 2.05.06 [12]. The tests on Charpy specimens demonstrated a sufficient level of residual impact toughness and cold resistance of the metal of pipe A (Table 2, 3), but its heating during the accident led to some decrease in the cold resistance of the base metal (Table 3).

The impact toughness of the factory welded joint (pipes B, C, notch along the fusion line) corresponds to the normalized value (Table 4). The impact toughness of the HAZ metal of the factory joint of this pipe at a different distances from the fusion line (0...20 mm) has almost the same values (at the level of ~ 210 J/cm²). It is

necessary to emphasize the low-impact toughness of the metal of the longitudinal weld (specimen 4). The strength of the circumferentially welded joint is at the level of strength of the base metal (655 MPa). The impact toughness of the metal of the site weld

and HAZ is also satisfactory. In general, it can be noted that the mechanical properties of the metal of the two investigated pipes meet the requirements of the specifications according to which they were manufactured.



Figure 5. Sharp bend of pipe A (templet 3/1) ~470 mm long and ~6,8 mm maximum depth
Slika 5. Oštra krivina cevi A (tempor 3/1) ~470 mm dužine i ~6,8 mm maksimalne dubine

Table 1. Chemical composition of pipe A, longitudinal and circumferential welds of pipeline fragments

Tabela 1. Hemijski sastav cevi A, uzdužni i obodni zavari fragmenata cevovoda

Marking	Mass fraction of elements, %											
	C	Mn	Si	S	P	Al	Ni	Mo	Ti	V	Nb	Cr
Pipe A	0.075	1.57	0.29	0.004	0.016	0.022	< 0.03	< 0.02	0.002	0.04	0.029	0.03
Longitudinal weld of the pipe	0.096	1.40	0.54	0.010	0.020	0.018	0.27	0.31	0.024	< 0.02	0.004	0.07
Circumferential weld of the pipe	0.075	1.41	0.21	0.013	0.040	0.012	0.07	0.31	0.005	< 0.02	0.007	0.05
TS 14-3-995 for the base metal	Not more than											
	0.12	1.70	0.50	0.010	0.020	0.050	-	0.30	-	0.080	0.06	-

Table 2. Mechanical properties of the base metal of the fractured pipes

Tabela 2. Mehanička svojstva osnovnog metala izlomljenih cevi

Area of cutting specimens (Fig.1), code	Base metal						
	Properties during rupture (GOST 1497, type II, III)					Impact toughness (GOST 9554, type I, II)	
	σ_y , MPA	σ_t , MPa	σ_y/σ_t	δ_5 , %	ψ , %	KCV ⁻¹⁵ , J/cm ²	KCU ⁻⁶⁰ , J/cm ²
Pipe A, Templet 3/2*	<u>533...535</u> 534	<u>600...600</u> 600	<u>0.89...0.89</u> 0.89	<u>23.2...23.5</u> 23.4	<u>69.8...69.8</u> 69.8	<u>138...155...163</u> 152	-
Requirements for the pipe metal [11]	441	588	0.9**	20	-	78.4	53.9

*Cylindric specimens

** Requirements HS&R 2.05.06

Note. The numerator indicates test values of all specimens, in the denominator average values are given

Table 3. Impact strength of the pipes (KCV, J/cm²)Tabela 3. Čvrstoća cevi na udar (KCV, J/cm²)

Specimens' cutting area, (according to Fig. 1)	Test temperature, °C				
	20	0	minus 15	minus 40	minus 60
Pipe A (near the edge of the fracture) 3/2	-	<u>176...201</u> 187	<u>163...179</u> 166	<u>120...140</u> 132	-
Pipe A (at a distance of 300 mm from the edge of the fracture), 3/2	<u>158...170</u> 163	<u>164...202</u> 183	<u>138...163</u> 152	<u>88...129</u> 115	-

Note. The numerator indicates minimum and maximum values, in the denominator average values are given

Table 4. Mechanical properties of welded joints

Tabela 4. Mehanička svojstva zavarenih spojeva

Area of cutting specimens (code)	Tensile tests	Tests on impact bending (GOST 6996, type IX, notch in the center of the weld)	Tests on impact bending (GOST 6996, type VI, IX, notch across HAZ)	
	σ_t , MPa	KCV ⁻¹⁵ , J/cm ²	KCV ⁻¹⁵ , J/cm ²	KCU ⁻⁶⁰ , J/cm ²
Circumferential weld (9/1)	<u>653...657</u> 655 (GOST 6996, type II)	<u>55.9...63.5...68.9*</u> 62.7	<u>34.0...64.7...69.8*</u> 56.2	<u>49.3...50.7...63.9**</u> 54.6
Pipe C, longitudinal weld (9/1)	<u>659...662</u> 660 (GOST 6996, type XIII)	-	-	-
Pipe B, longitudinal welded joint (4)	-	<u>24.4...29.2...33.9</u> 29.2	<u>85...97...108.0</u> 96.6	<u>107...225.6...309.2</u> 214.0
Requirements of TS 14-3-995 to the metal of factory welded joints	Not lower than the strength of the base metal	-	-	39.2

*The notch was produced along the weld or throughout the area of the facing layer

**The notch was produced in the center of the root weld of the specimens 3, 3/2, 2, (pipe A), 4 (pipe B) 9/1, 9 (pipe C)

3.5. Structural characteristics of the pipe metal and welded joints

As is seen from Fig. 6, the structure of the metal of pipe A (specimens 3) near the edge of the rupture was formed as a result of heating the metal at a temperature close to the stabilizing temperature (Fig. 6a). But already at a distance of

~300 mm from the edge of the rupture, the pipe metal was heated faster to the tempering temperature (Fig. 6b). The fact of softening as a result of structural transformation is confirmed by an increased hardness of the base metal: the hardness of the metal of pipe A is (175-180) HV.

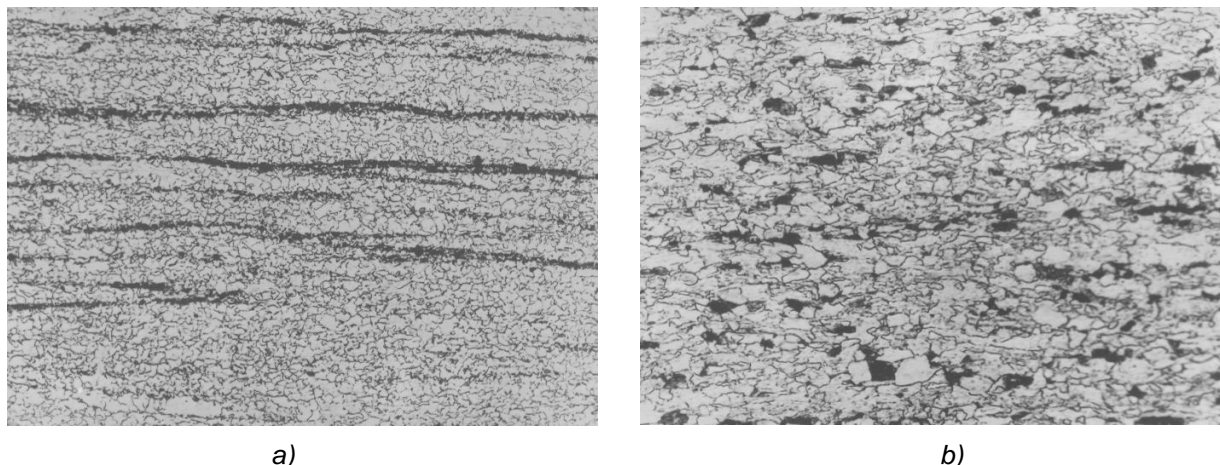


Figure 6. Microstructure of pipe A, $\times 320$: a – near the fracture edge; b – at the distance 300 mm from the fracture edge

Slika 6. Mikrostruktura cevi A, $\times 320$: a – u blizini ivice loma; b – na udaljenosti 300 mm od ivice loma

The metal of the longitudinal welded joint of the pipe B, as well as the base metal, was subjected to heat, because both the metal of the weld as well as of heat-affected zone (area of a coarse grain) underwent a structural transformation (Fig. 7b).

The structure of the circumferential site joint (specimens 9/1) consists of an acicular and polygonal ferrite in the form of a column appearance and individual polyhedral grains. The area of a coarse grain represents a mixture of a lower and upper bainite, as well as a ferritic component on the grain boundaries (Fig. 7c). The size of a coarse grain mainly corresponds to the number 4 according to GOST 5639. The length of the zone of a coarse grain is up to 0.4 mm. It can be emphasized that the fracture, which was recorded in the area near the facing layer (at a length of 130 mm, specimens 9/1), occurred outside the area of a coarse grain, which is the most brittle in the HAZ of welded joints. The hardness of the metal of the facing layer is about 215 HV, and the maximum hardness in the area of a coarse grain reaches 236 HV.

The contamination of steel with non-metallic inclusions in all investigated pipes is insignificant (1 point as to oxides content according to GOST 1778). Separate slag inclusions,

elongated inclusions (sulfides, oxides) were not revealed.

3.6. Structural characteristics of the metal in the crack zone

Metallographic examinations of structural features of the metal areas were carried out in the zone of crack colonies located near the main crack in order to estimate the nature of their origin. The analysis of microsections cut perpendicular to the trajectory of the crack propagation, showed that their depth is small (not more than 0.2 mm). The faces of the cracks are almost parallel to each other. The bottoms of the cracks are rounded, and their walls are smooth without branching, which is typical to the corrosion process occurred through a mechanism of a local anodic dissolution. Closer to the edge of the fracture, in the zone of deformation (thinning of the pipe wall during fracturing), such cracks almost have no ruptures and did not propagate into the depth (Fig. 8a).

Microstructure of the metal of the longitudinal welded joint of the pipe B, which was not in the zone of gas burning (specimens 9/1), is typical for pipe welded joints of X70 steel (Fig. 7a) and consists of an acicular and polygonal ferrite. The hardness of the outer weld is within 225-227 HV, and the inner one is 240-245 HV.

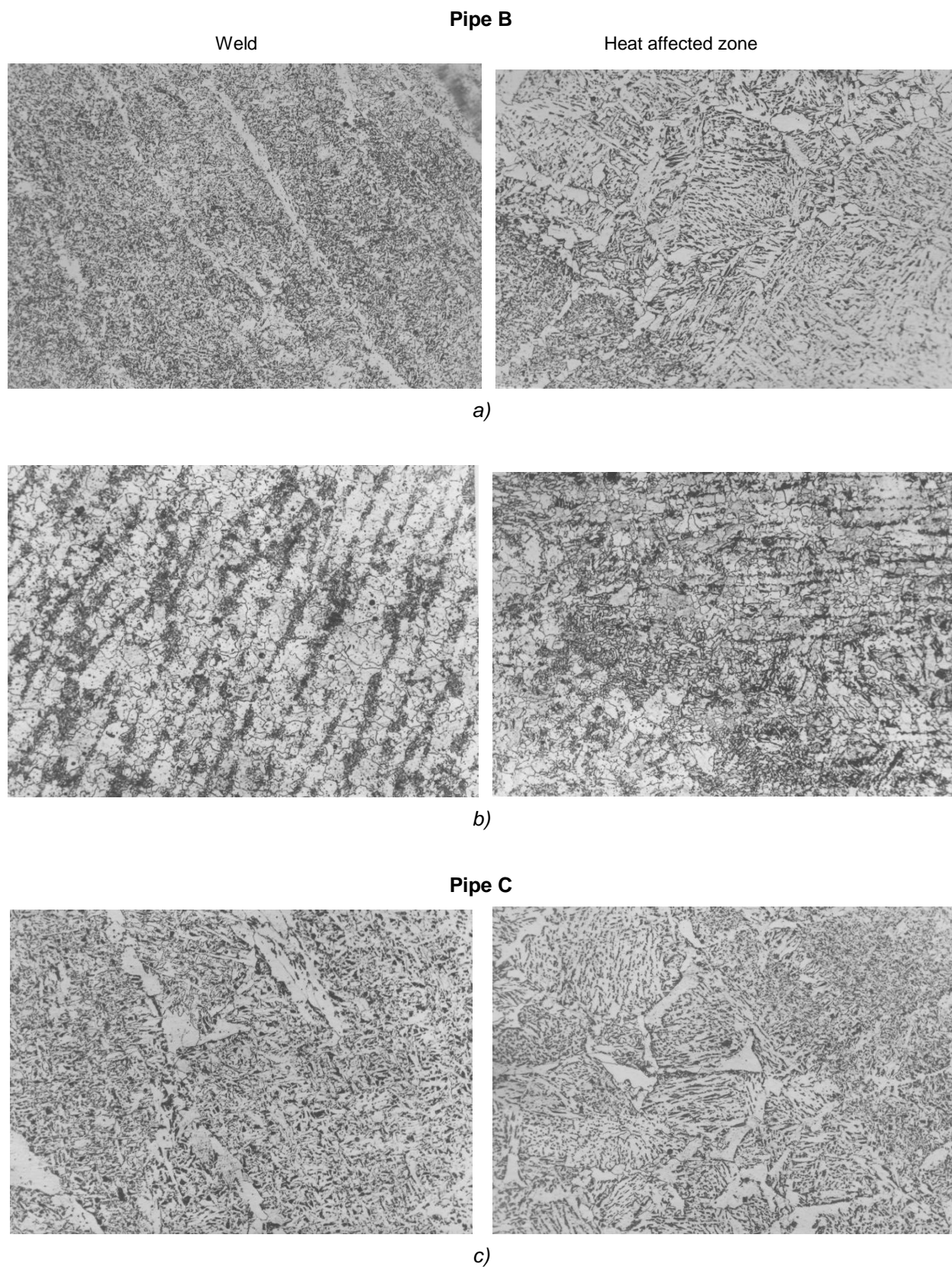


Figure 7. Microstructure of the longitudinal (a, b) and girth (c) welds of the pipes, $\times 320$

Slika 7. Mikrostruktura uzdužnih (a,b) i prstenastih (c) šavova cevi, $\times 320$

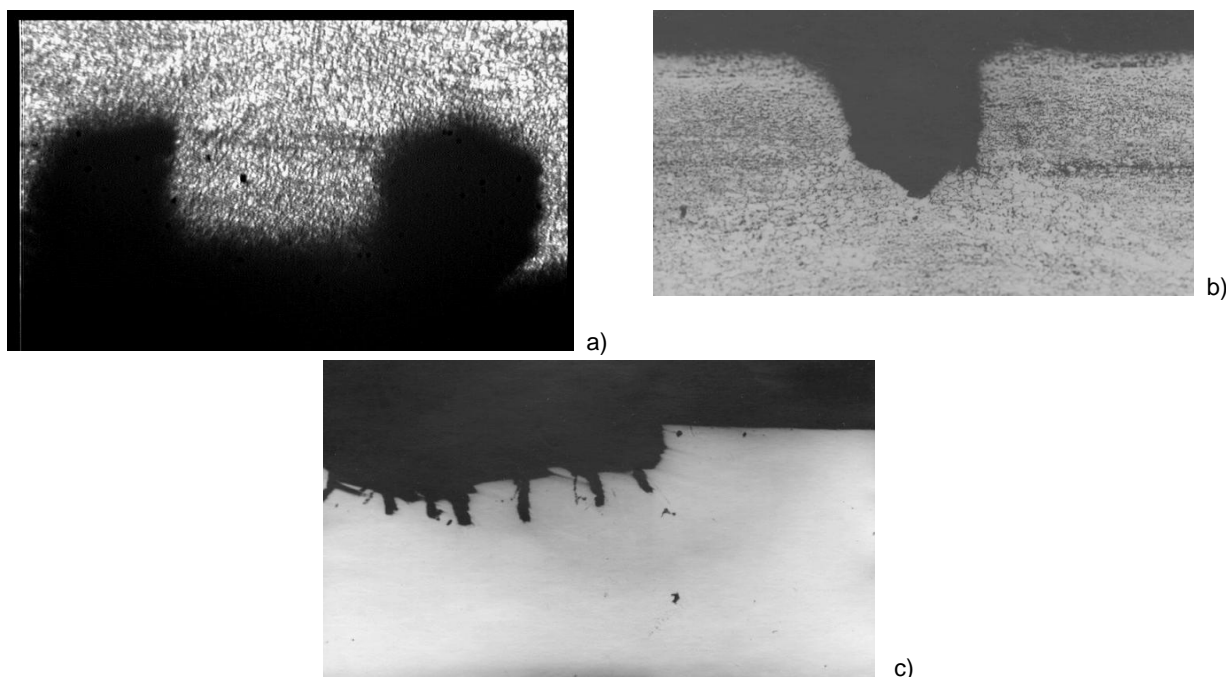


Figure 8. Micro polished sections: a – cracks at the distance ~20 mm from break edge, $\times 200$;
c – crack at the distance ~10 mm from break edge, $\times 100$

Slika 8. Mikropolirani profili: a – pukotine na rastojanju ~20 mm od ivice loma, $\times 200$;
c – pukotina na udaljenosti ~10 mm od ivice loma, $\times 100$

In the heat-affected zone of the outer weld on the area of a coarse grain, the structure consists mainly of an upper bainite with a polygonal ferrite on the boundaries of austenitic grains (Fig. 7b). The grain size in the mentioned area corresponds to the number 4 according to GOST 5639. The hardness of the metal in this area is 219-225 HV.

3.7. Estimation of soil corrosivity

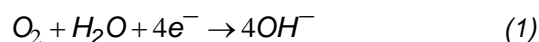
The ion composition of the soil from the accident site is represented by cations Ca^{2+} (20.0 mg/l), Mg^{2+} (10.9 mg/l), and anions Cl^- (16.0 mg/l), SO_4^{2-} (32,3 mg/l), HCO_3^- (115.9 mg/l) with a dry residue 128 mg/l, highly alkaline pH 8.6 (more than 8.5) and humidity 29.5 %. The corrosion rate, measured by the method of polarization resistance, in the water extract from soil is 0.13 mm/year. According to the standard documents of Ukraine, the soil corrosivity was estimated with respect to X70 steel: pH (from 8.5 to 14), corrosion rate (from 0.01 to 0.3 mm/year) indicate that soil is a medium with an average corrosivity, humidity (from 15 to 20 %) is with a high corrosivity.

3.8. Slow strain rate tests

Stress corrosion cracking of X70 steel was investigated in the model soil electrolyte at

protective potentials without an ohmic component - 0.75 V, -1.05V in and -1.2 V at periodic immersion [13,14].

In almost neutral NS4 solution under cathodic polarization, the following main reactions occur on steel:



In the presence of hydrocarbonate ions in the solution, iron carbonate is formed:



Under such conditions (pH 8.2), the layer of FeCO_3 is porous and loose, its protective properties are low, so the passivation of the steel surface was not observed (Fig. 9).

According to the results of electrochemical, corrosion-mechanical studies and fractographic examinations (Fig. 9-11), ranges of potential were established, in which the mechanism of SCC is varied. At the potentials that are more positive than -0.75 V, corrosion cracking occurs mainly through a mechanism of a local anodic dissolution (Fig. 8), the specimens are featured by a tough morphology of fracture (Fig. 10).

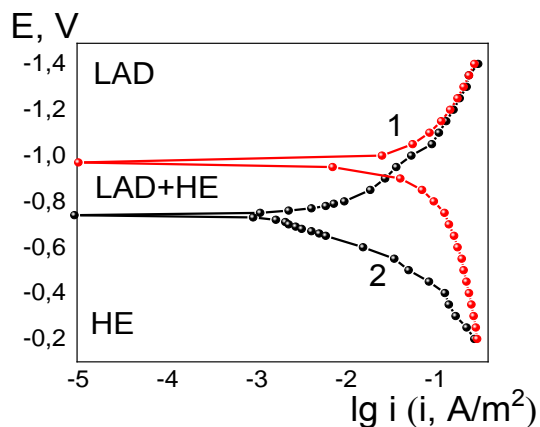


Figure 9. Polarization curves at different scanning potential rate (1 – 0.5 mV/s; 2 – 200 mV/s). LAD – local anodic dissolution; HE – hydrogen embrittlement

Slika 9. Polarizacione krive pri različitim brzinama potencijala skeniranja (1 – 0,5mV/s; 2 – 200mV/s). LAD – lokalno anodno rastvaranje; HE – vodonična krtoš

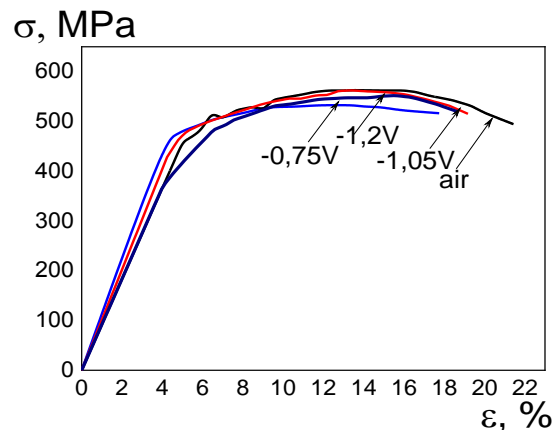
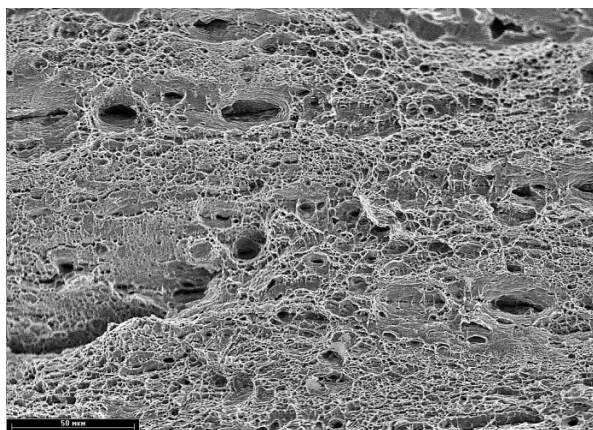
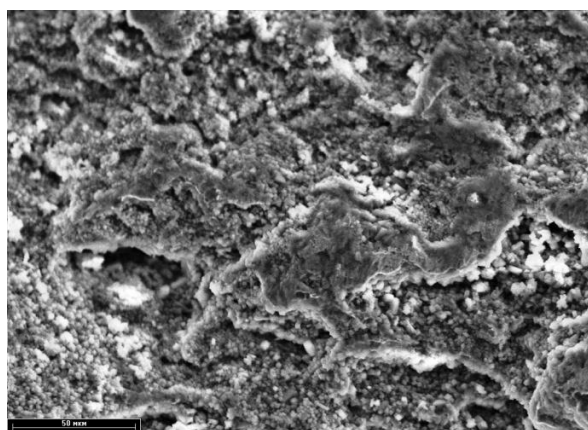


Figure 10. The curves of mechanical fracturing of X70 steel specimens in air and corrosion-mechanical fracturing in the solution at different potentials

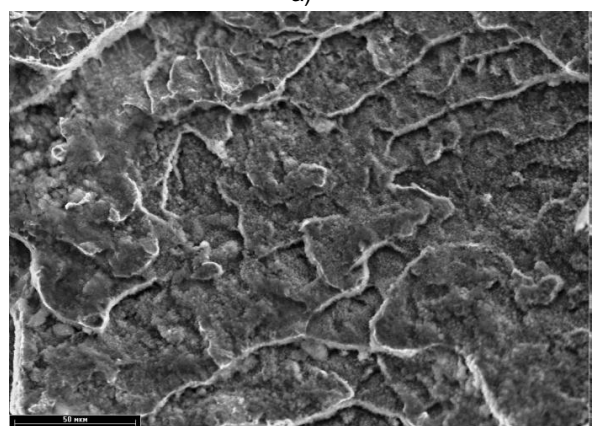
Slika 10. Krive mehaničkog lomljenja uzoraka čelika X70 na vazduhu i koroziono-mehaničko lomljenje u rastvoru pri različitim potencijalima



a)



b)



c)



d)

Figure 11. Fractured specimens and morphology of breaking surface after testing in air (a) and solution at potentials: b – $E = -0.75$ V; c – $E = -1.05$ V; d – $E = -1.2$ V

Slika 11. Slomljeni uzorci i morfologija površine lomljenja nakon ispitivanja na vazduhu (a) i rastvoru na potencijalima: b – $E = -0,75$ V; c – $E = -1,05$ V; d – $E = -1,2$ V

In the range of potentials from -0.75 to -1.05 V, a local anodic dissolution and hydrogen embrittlement occur simultaneously and this fact correlates with a decrease in the plastic properties of steel and up to 15...30% increase in the fraction of quasi brittle delaminations in the fracture morphology (Fig. 11). In the range of potentials, which are more negative than -1.05 V, the mechanism of corrosion cracking is hydrogen embrittlement with a subsequent loss of ductile properties by the metal and an increase in the fraction of quasi brittle delaminations in the fracture morphology (Fig. 11).

4. CONCLUSIONS

1. It was found that the accident on the section of the main gas pipeline was initiated by a stress-corrosion defect of ~ 470 mm length with the maximum depth of ~ 6.8 mm, oriented in the direction of the generatrix of the pipe and perpendicular to its outer surface, whose propagation deep inside the pipe wall occurred through a mechanism of a local anodic fracture in the elastic region.

2. The formation of a stress-corrosion crack is caused by a damage to the protective tape coating of the pipe, a high corrosivity of the soil at the site of the accident (soil humidity is 29 %, corrosion rate is 0.13 mm/year) and a complex stress-strain state as a result of natural conditions (swamp and ravine).

3. The metal of the fractured pipe of the gas pipeline of X70 steel meets the requirements of TS 14-3-995 as to mechanical characteristics, ultimate strength, impact toughness and relative elongation. Softening of the metal near the rupture line is predetermined by heating of the pipe to the stabilizing temperature as a result of gas burning. The tests of the Charpy- specimens on impact bending demonstrated a sufficient level of residual impact toughness and cold resistance of the metal of all pipes.

4. Microstructure of steel is typical for the steel of controlled rolling, some structural transformations were noted that were caused by heating of the pipe during the accident. The microstructure of the metal of longitudinal and circumferential welds is typical for the pipe welded joints of X70 steel, produced with the use of welding materials used during construction of the gas pipeline.

5. According to the results of a complex of electrochemical, corrosion-mechanical and fractographic examinations, the existence of three ranges of potentials was established, in which stress-corrosion cracking occurs: at the potentials, which are more positive than -0.75 V, corrosion cracking occurs mainly through a mechanism of a

local anodic dissolution, in the range of potentials from -0.75 to -1.05 V, a local anodic dissolution and hydrogen embrittlement occur simultaneously, at the potentials, which are more negative than -1.05 V, the mechanism of corrosion cracking is hydrogen embrittlement.

Acknowledgements

The work was carried out by support of the National Academy of Sciences of Ukraine in 2020-2021 (State registration number 0121U110555).

5. REFERENCES

- [1] A.I.Pyatnichko, T.K.Krushnevich (2008) The main directions of improvement of the gas transportation system of Ukraine, *Technical gases*, 3, 9-14.
- [2] A.Ya.Krasovskii, I.V.Lokhman, I.V.Orynyak (2012) Stress-corrosion failures of main pipelines, *Strength of Materials*, 44, 129-143.
- [3] B.N.Leis (1991) Some aspects of stress-corrosion-cracking analysis for gas transmission pipelines, *Materials Performance Maintenance*, p.107-121.
- [4] C.I.Ossai, B.Boswell, I.J.Davies (2015) Pipeline failures in corrosive environments – A conceptual analysis of trends and effects, *Engineering Failure Analysis*, 53, 36-58.
- [5] Y.Zhao, M.Song (2016) Failure analysis of a natural gas pipeline, *Engineering Failure Analysis*, 63, 61-71.
- [6] P.J.Kentish (1985) Gas pipeline failures: Australian experience, *British Corrosion Journal*, 20(3), 139-146.
- [7] S.A.Kotrechko, A.Y.Krasovskii, Y.Y.Meshkov, Y.A.Polushkin, V.M.Torop (2002) Influence of long-term operation on the toughness of 17GS pipeline steel, *Strength of Materials*, 34(6), 541-547.
- [8] H. Nykyforchyn, L.Unigovskyi, O.Zvirko, O. Tsyurulnyk, H.Krechkovska (2021) Pipeline durability and integrity issues at hydrogen transport via natural gas distribution network, *Procedia Structural Integrity*, 33, 646-651.
- [9] A.Ya. Krasovskii, I.V. Orynyak, (2010) Strength and reliability of piping systems, *Strength of Materials*. 42(5), 613-621.
- [10] S.G.Polyakov, A.A.Rybakov (2009) The main mechanisms of stress corrosion cracking in natural gas trunk lines, *Strength of Materials*, 41(5), 456-463.
- [11] TS 14-3-995-81 Steel electric welded pipes with longitudinally weld expanded 1420 mm in diameter from the X-70 grade steel. Technical specifications.
- [12] BR 2.05.06-85 Building regulations. PIPE MAINS
- [13] L.Nyrkova (2020) Stress-corrosion cracking of pipe steel under complex influence of factors *Engineering Failure Analysis*, 116, 104757.
- [14] L.I.Nyrkova, A.O.Rybakov, S.O.Osadchuk, S.L. Melnichuk, N.O.Hapula (2014) Method for tests of sensibility of pipe steels to stress-corrosion cracking from the influence of alternating wetting. Patent for invention No. 107381, publ. 10.12.2014, bull. № 2.

IZVOD

ANALIZA UZROKA LOMA MAGISTRALNOG GASOVODA

Sproveden je kompleks istraživanja za utvrđivanje uzroka havarije magistralnog gasovoda od čelika 1420x15,7 mm X70 nakon 20 godina rada. Utvrđeno je da je destrukciju cevi inicirala uzdužna pukotina dužine 470 mm i maksimalne dubine 6,8 mm, orijentisana u pravcu cevi i okomita na spoljašnju površinu cevi koja je identifikovana kao prslina od naponske korozije. Nastanak pukotine je usled odvajanja zaštitnog premaza trake, visoke aktivnosti korozije tla i složenog naponsko-deformacionog stanja uzrokovanog odstupanjima od projektnih ciljeva tokom izgradnje. Hemijski sastav osnovnog metala svih ispitivanih cevi odgovara zahtevima tehničkih uslova za čelične cevi kategorije X70; zavarivanje cevi se izvodi tipičnim materijalima koji se koriste u postrojenjima za zavarivanje cevi. Uprkos razlikama, strukturne i mehaničke karakteristike (napor tečenja, krajnja čvrstoća i udarna čvrstoća) čelika i metala šava ispitivanih cevi su identične. Relativno izduženje ($\bar{\delta}_5$) ispitivanih cevi je ispod normalizovanih vrednosti, ali je potrebno uzeti u obzir mogućnost odstupanja ovih karakteristika čelika u početnom stanju. Značajne rezerve žilavosti indirektno ukazuju na nisko oštećenje metala i, shodno tome, na zadovoljavajuću otpornost na destrukciju metala ispitivanih cevi.

Ključne reči: magistralni cevovod, čelik X70, mikrostruktura, mehanička svojstva, naponsko-koroziono pucanje, katodna zaštita

Naučni rad

Rad primljen: 01. 01. 2023.

Rad prihvaćen: 31. 01. 2023.

Rad je dostupan na sajtu: www.idk.org.rs/casopis